

Three-body interactions, scaling variables, and singular diameters in the coexistence curves of fluids

M. W. Pestak*

Department of Physics, The Pennsylvania State University, University Park, Pennsylvania 16802

Raymond E. Goldstein

*Laboratory of Atomic and Solid State Physics and Materials Science Center, Clark Hall, Cornell University,
Ithaca, New York 14853-2501*

M. H. W. Chan

Department of Physics, The Pennsylvania State University, University Park, Pennsylvania 16802

J. R. de Bruyn and D. A. Balzarini

Department of Physics, The University of British Columbia, Vancouver V6T 2A6, British Columbia, Canada

N. W. Ashcroft

*Laboratory of Atomic and Solid State Physics and Materials Science Center, Clark Hall, Cornell University,
Ithaca, New York, 14853-2501*

(Received 29 January 1987)

Evidence is presented that the pair-potential model of fluids is insufficient in the critical region. In particular, data on the critical properties of Ne, N₂, C₂H₄, C₂H₆, and SF₆ are shown to exhibit well-defined trends in the variation of certain nonuniversal critical amplitudes with the critical temperature T_c . Both the slope of the coexistence-curve diameter far from the critical point, and the deviations from linear behavior which appear closer to T_c , increase systematically with T_c , and are directly correlated with the molecular polarizability. These trends are explained on the basis of the increasing importance of three-body dispersion (Axilrod-Teller) forces in the more polarizable systems, and a simple mean-field theory is developed which accounts for the observed correlations. The possibility of incorporating the effects of three-body interactions into an effective pair potential is explored within the context of perturbation theory in the grand canonical ensemble, and it is shown that such an interaction is explicitly a function of fugacity. In the critical region, this is equivalent to a thermal scaling field which depends on the bare chemical potential of the system, and ultimately leads to a breakdown in the classical law of the rectilinear diameter. The magnitude of this field mixing, and hence of the diameter anomaly, scales with the product of the particle polarizability and the critical number density, in agreement with experiment.

I. INTRODUCTION

In theories of second-order phase transitions, it is often possible to describe the singular behavior of complex systems in terms of the known properties of simpler ones, but with a change of scaling variables. Such a transcription is exact in the case of decorated lattice gases,^{1,2} can hold within the context of a low-order perturbation theory,³ or may simply be advanced as a working hypothesis in a phenomenological approach (the "smoothness postulate"⁴). A well-studied case involving this change of variables is the relation of the liquid-vapor critical point of a simple fluid to the critical point of the spin- $\frac{1}{2}$ Ising ferromagnet.

While symmetry considerations dictate that the scaling variables in a magnetic system described by an Ising model are the reduced temperature and magnetic field, the lack of a rigorous particle-hole symmetry in a fluid suggests that some asymptotically linear combination of reduced temperature and the shift of the chemical potential from its value on the critical isochore may be more ap-

propriate at the liquid-vapor critical point. Certain exactly solvable lattice^{5,6} and continuum models⁷ do exhibit such "revised"^{8,9} scaling variables, but, at least in the former, it is the structure of the underlying lattice rather than the governing Hamiltonian which is responsible for the broken symmetry. In general these models provide no truly *microscopic* basis for an understanding of the issue of particle-hole symmetry in fluids. On the other hand, renormalization-group treatments¹⁰ of a generalized Landau-Ginzburg-Wilson Hamiltonian do attribute this so-called *field mixing* to asymmetric operators in a field-theoretic Hamiltonian, and in particular to those terms which contain cubic and higher odd powers of the order parameter and its gradients.

Irrespective of the origin of field mixing, a common prediction of such theoretical approaches is the existence of a weak singularity in the average of the densities of the coexisting phases, a breakdown of the classical law of the rectilinear diameter.¹¹ We review in Sec. II the mechanism underlying the prediction that, for a one-component fluid, the coexistence-curve diameter ρ_d behaves like

$$\rho_d \equiv \frac{\rho_l + \rho_v}{2\rho_c} = 1 + A_{1-\alpha} t^{1-\alpha} + A_1 t + \dots, \quad (1)$$

where ρ_l and ρ_v are the densities of the coexisting liquid and vapor phases, ρ_c is the critical density, and the reduced temperature is $t = (T_c - T)/T_c$. A value of $A_{1-\alpha} \neq 0$ would indicate field mixing, α (≈ 0.11) being the exponent which characterizes the power-law divergence of the constant-volume specific heat at the critical point. Far away from the critical point, the linear-temperature variation described by the third term in (1) is universally observed.

In spite of intense experimental study over many years, most fluids actually seem to show *no* measurable deviations from analytic behavior,¹² and the evidence of anomalies with the predicted exponent is weak in the case of *insulating* fluids such as the rare gases, and in binary mixtures.¹³ To date, the strongest evidence in any *non*-conducting fluid is found in SF₆, as reported by Weiner, Langley, and Ford,¹⁴ and further analyzed by Ley-Koo and Green.¹⁵ A quantitative analysis to show the presence of a singular term of the form in Eq. (1) is difficult since the exponent $1-\alpha \approx 0.89$ and is thus sufficiently close to unity to make a clear distinction between the singular and linear terms problematic. There are, in addition, corrections to scaling terms with exponents only slightly larger than unity, which become important at larger t . Given data over a wide range of reduced temperatures, it should be possible in principle to separate out the contributions of these different terms; however, the strongly divergent compressibility near the critical point introduces gravitational rounding of the transition.¹⁶ Even for a very thin fluid sample (~ 1 mm) this rounding effect becomes severe for $t \leq 2 \times 10^{-4}$. There is thus a very limited temperature range within which a deviation from an analytic diameter may be observed.

On the other hand, recent high-precision measurements¹⁷ of the liquid-vapor coexistence curves of the metals cesium and rubidium have demonstrated that remarkably large anomalies do exist in the simple metals, and with the expected critical exponent. In view of the fact that these fluids are *metallic* in their critical regions, it has been suggested¹⁸ that the many-body effects present in systems with delocalized electrons, in particular those associated with electronic screening, lead to the same type of field mixing as found in the solvable lattice models.

It is therefore natural to ask if there exist many-body effects in insulating fluids which would influence the scaling variables in a similar manner, and this paper is an account of both theoretical and experimental studies which suggest that similar effects are indeed present. We report¹⁹ on analyses of coexistence-curve data for several simple fluids, Ne, N₂,²⁰ C₂H₄,²¹ C₂H₆,²² and SF₆,¹⁴ and show that there are striking trends in the properties of the diameters of these systems. Both the slope of the linear temperature dependence far away from the critical point [the coefficient A_1 in Eq. (1)] and the amplitude of the deviation from that linear behavior at smaller reduced temperature scale systematically with the critical temperature. The former is in contrast with the expectations of classical theories such as the van der Waals theory, which predict

a universal slope of the diameter. The fact that these substances, in particular the spherically symmetric systems among them, do not satisfy exactly a law of corresponding states suggests that there is some new energy scale in the problem, distinct from that set by two-body dispersion forces.

In Sec. III we propose that this new scale is set by the strength of many-body forces, and in particular by *three-body forces*. It is known from comparison of gas-phase atom-atom scattering data and condensed-phase properties that many-body forces contribute at the level of 10–15% to the bulk cohesive energies of rare-gas liquids and solids.²³ Since triplet interactions involve an odd number of density operators in the Hamiltonian, it is not surprising that their presence may have an important effect on the coexistence-curve diameter, whose behavior is sensitive to the liquid-vapor symmetry of the fluid. Among the many-body forces which have been studied, the three-body dispersion forces of the form derived by Axilrod and Teller²⁴ (AT) are usually the dominant ones, although three-body exchange interactions are important in the lighter, less polarizable substances.²⁵ That such interactions are expected *a priori* to introduce a new energy scale can be seen in the form of the AT potential; for a triad of particles at $(\mathbf{r}_1, \mathbf{r}_2, \mathbf{r}_3)$ with θ_i the vertex angles of the triangle they form

$$V_{\text{AT}}(\mathbf{r}_1, \mathbf{r}_2, \mathbf{r}_3) = V_3^0 \frac{[3 \cos(\theta_1) \cos(\theta_2) \cos(\theta_3) + 1]}{r_{12}^3 r_{13}^3 r_{23}^3}, \quad (2)$$

where the amplitude is $V_3^0 \sim I\alpha_p^3$, with I the energy of the first excited electronic state, usually approximated by the ionization potential, and α_p the polarizability (the subscript of which distinguishes it from the critical exponent α). In contrast, the two-body dispersion force is, at long range,

$$V_2 = -\frac{V_2^0}{r_{12}^6}, \quad (3)$$

where $V_2^0 \sim I\alpha_p^2$. The relative importance of the triplet interactions thus scales like

$$\frac{V_3}{V_2} \sim \frac{\alpha_p}{\bar{r}^3} \sim \alpha_p \rho, \quad (4)$$

where \bar{r}^3 is a mean-cubed interparticle spacing in the fluid, and is proportional to the volume per particle, or the inverse of the number density ρ . We thus conclude that an appropriate measure of the relative strength of triplet potentials at the critical point is given by the dimensionless *critical polarizability product*

$$\alpha_p \rho_c, \quad (5)$$

with ρ_c the critical number density. The values of this parameter for the systems considered in this paper are shown in Table I, where it is seen that its variation from Ne to SF₆ is about a factor of 3. The corresponding increase in critical temperature is roughly an order of magnitude, consistent with the general notion that T_c scales with the strength of the two-body interaction, and hence like $(\alpha_p \rho_c)^2$. That $\alpha_p \rho_c$ itself increases like $T_c^{1/2}$ means

TABLE I. Critical parameters and critical polarizability products $\alpha_p \rho_c$.

Fluid	T_c (K)	P_c (dyne/cm ²)	n_c (g cm ⁻³)	α_p (Å ³)	$\alpha_p \rho_c$
HD	35.9569	1.506×10^7	0.0481	0.798	0.00764
Ne	44.4789	2.72	0.484	0.396	0.00571
N ₂	126.2143	3.398	0.314	1.74	0.0117
C ₂ H ₄	282.3768	5.040	0.215	4.25	0.0196
C ₂ H ₆	305.2692	4.194	0.206	4.50	0.0186
SF ₆	318.707	3.759	0.733	6.54	0.0198

that three-body interactions are relatively more important in more polarizable fluids with correspondingly higher critical temperatures. In mean-field theory, the contribution of n -body dispersion forces to the pressure is, in general, proportional to $(\alpha_p \rho)^n$, and for the systems considered here, with relatively small $\alpha_p \rho_c$, we may restrict attention to $n \leq 3$, that is, to the first-order corrections to pairwise additivity.²⁶

We discuss in Sec. III a simple mean-field calculation which predicts that the diameter slope, outside of the asymptotic critical region, increases linearly with $\alpha_p \rho_c$, and the experimental data discussed in Sec. IV confirm this. It is significant that the slope *increases* with the critical polarizability product, for this is consistent with a primarily *repulsive* three-body potential, such as the Axilrod-Teller interaction. We find that the critical compressibility factor and the amplitude of the order-parameter singularity near the critical point also vary linearly with $\alpha_p \rho_c$, in a way which is completely consistent with the mean-field results. The existence of correlations between such quantities has been noted before,⁶ but is here explained for the first time on a microscopic level.

The fact that the same systematic trend appears in the magnitude of the deviations from linear behavior of the diameter which appear at smaller reduced temperature as in the slopes far away from the critical point suggests that they have the same origin. It has been suggested by Reatto and Tau²⁷ that, within a coarse-grained description, the effective Landau-Ginzburg-Wilson Hamiltonian of a fluid with triplet interactions has the same form as the asymmetric model studied by Nicoll *et al.*¹⁰ General field-theoretic arguments relevant to that Hamiltonian show that the presence of certain cubic and quintic operators leads to a revision in scaling variables. From a more global perspective, we suggest in Sec. II that *revised scaling variables may be seen as consequences of effective intermolecular potentials which depend on thermodynamic fields*, and we thus consider in Sec. III how three-body interactions may be incorporated into effective pair potentials which are thermodynamic state dependent. We develop this notion within the context of the theory of fluids by deriving an effective potential which is an explicit function of the *fugacity* of the system. This mapping is examined in more detail in a separate analysis²⁸ dealing with certain lattice models, which confirms the basic ideas advanced here.

Section IV is a discussion of the experimental results, and of their consistency with the theory outlined in Sec.

III. In the conclusion, Sec. V, we pose questions about higher-body interactions and quantum effects at the critical points of fluids.

II. FIELD MIXING

A useful starting point for the discussion of the concept of thermodynamic field mixing is the phenomenological form proposed by Rehr and Mermin⁸ of the scaling equation of state for a one-component fluid in the critical region. The critical behavior of the pressure P , as a function of reduced temperature t and the shift of the chemical potential from its value on the chiral isochore $\mu \equiv \mu(T, \rho) - \mu(T, \rho_c)$, is postulated to scale as originally proposed by Widom,²⁹ but with revised scaling variables:

$$P(\mu, t) = P_0(\zeta, \tau) + \tau^{2-\alpha} f_{\pm}(\zeta/\tau^{\beta\delta}). \quad (6)$$

Here P_0 is a smooth background term, and $\tau = \tau(\mu, t)$ and $\zeta = \zeta(\mu, t)$ are the effective temperature and field, analytic in their arguments. The scaling functions $f_{\pm}(z)$, for supercritical and subcritical states, are those of a system having all of the usual symmetry properties associated with a Hamiltonian possessing asymptotic "particle-hole" symmetry; e.g., $f(0_-) = f(0_+)$, $f'(0_-) = -f'(0_+)$, etc., where a prime indicates differentiation with respect to the argument z . The exponents α , β , and δ are also those of a symmetric system. The thermodynamic densities $\rho_{\pm} = (\partial P / \partial \mu)_T$ from the two branches of the coexistence curve $\zeta = 0^{\pm}$ are found to be

$$\rho_{\pm} = \rho_c \pm f'_{-}(0) \left(\frac{\partial \zeta}{\partial \mu} \right) \tau^{\beta} + (2-\alpha) f_{-}(0) \left(\frac{\partial \tau}{\partial \mu} \right) \tau^{1-\alpha} + O(\tau). \quad (7)$$

The mean density $\bar{\rho} = (\rho_- + \rho_+)/2$ thus deviates from the critical density as

$$\bar{\rho} = \rho_c + (2-\alpha) f_{-}(0) \left(\frac{\partial \tau}{\partial \mu} \right) \tau^{1-\alpha} + \dots \quad (8)$$

The weak singularity in the diameter arises thus from the mixing of the one-body operator μ into the thermal scaling field τ . The analytic background P_0 will contribute a term linear in t which, far away from the critical point, gives rise to the analytic diameter seen nearly universally in fluids. As shown in Fig. 1, the extrapolation of this analytic diameter to $t=0$ suggests a critical density ρ'_c which

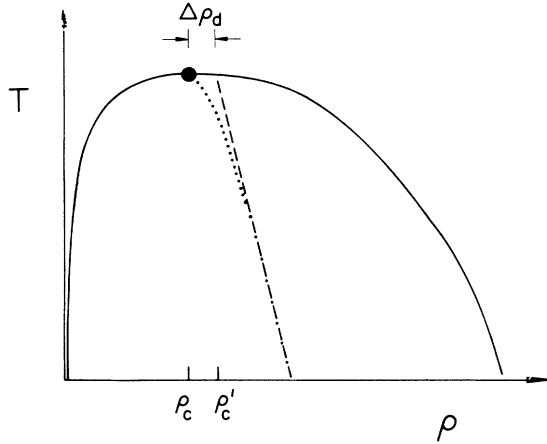


FIG. 1. Schematic illustration of a liquid-vapor coexistence curve, indicating the deviation of an analytic extension of the linear diameter from the true singular diameter.

differs from the true ρ_c by an amount $\Delta\rho_d$. Equation (8) indicates that $\Delta\rho_d \sim \partial\tau/\partial\mu$.

Another consequence of field mixing is a divergence in the difference between the liquid and vapor compressibilities,⁹ which is found by differentiating Eq. (7) and then setting $\zeta=0^\pm$:

$$\left[\frac{\partial\rho}{\partial\mu} \right]_{\text{liq}} - \left[\frac{\partial\rho}{\partial\mu} \right]_{\text{vap}} = 4\beta f''(0) \left[\frac{\partial\zeta}{\partial\mu} \right] \left[\frac{\partial\tau}{\partial\mu} \right] \tau^{\beta-1} + \dots, \quad (9)$$

the ellipsis standing for less singular terms. In either phase, the compressibility itself has a leading divergence of the form $\tau^{-\gamma}$. From Eqs. (8) and (9), this phenomenological theory predicts that if the diameter anomaly is toward lower densities, as in Fig. 1, i.e., $\partial\tau/\partial\mu > 0$, then the liquid-phase compressibility will be *greater* than that of the vapor phase. In Sec. IV we discuss the experimental status of this prediction.

This phenomenological derivation of the singular diameter is in the context of an equation of state appropriate to the *asymptotic* behavior of the free energy near the critical point, but is in fact motivated by lattice models^{5,6} which show field mixing over the *entire* phase diagram. A typical *decorated* lattice, shown in Fig. 2, consists of a primary lattice of spins on whose bonds reside the statistical systems which comprise the secondary lattice. As a consequence of the one-dimensional coupling of the decorating spins to those of the primary lattice, the statistical traces over the degrees of freedom of the former may be performed explicitly and independently, since by construction there are no couplings between the secondary sites.

For decorated-lattice magnetic models, let $F(\{K\}, H)$ be the free energy per site of the model with N sites, where H and $\{K\}$ are, respectively, the magnetic field and a set of bare coupling constants. The general relationship between F and the free energy F_I of the nearest-neighbor Ising model is

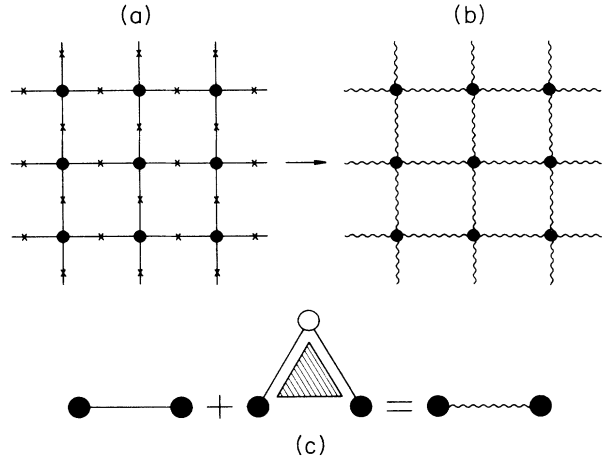


FIG. 2. Decorated-lattice transformation in two dimensions, and its similarity to the definition of an effective pair potential which accounts for triplet interactions. The original lattice (a) consists of primary vertex sites and secondary sites on the lattice bonds. After tracing over the latter, there remains a primary lattice (b) coupled via effective interactions (wiggly lines). (c) The effective two-body potential ϕ_{12} (wiggly line) is given by a statistical trace over a third particle (open circle) which is coupled to the two particles through a pair potential (solid line) and a triplet potential (shaded triangle).

$$F(\{K\}, H) = F_I[K_I(\{K\}, H), H_I(\{K\}, H)] + G(\{K\}, H). \quad (10)$$

The effective nearest-neighbor coupling K_I , magnetic field H_I , and additive term G are all *analytic* functions of their arguments, for they are related to the conditional partition functions of the three-spin system on a lattice bond, which, by virtue of being *finite* systems, necessarily have no singular thermodynamic behavior at finite temperature.

In a way completely analogous to its derivation within the scaling approach above, the mean magnetization $\bar{M} = (M_+ + M_-)/2$, with $M_\pm = (\partial F/\partial H)$, is thus

$$\bar{M} = \left[\frac{\partial G}{\partial H} \right]_{\text{coex}} + E_I \left[\frac{\partial K_I}{\partial H} \right]_{\text{coex}}, \quad (11)$$

where $E_I = (1/N) \langle \sum_{\langle ij \rangle} s_i s_j \rangle_I$ is the nearest-neighbor spin correlation of the Ising model; and the subscript “coex” means the condition $H_I \rightarrow 0^\pm$.

It now follows that the presence of a weak singularity in the diameter arises from the mixing of energylike terms into the thermodynamic derivative which yields the density, for in Eq. (11), it is the *nearest-neighbor* spin-spin correlation function E_I which has a $t^{1-\alpha}$ singularity (since the $H=0$ specific heat diverges with a power law $t^{-\alpha}$).

The above discussion of magnetic systems also applies of course to the lattice-gas model of fluids. Turning now to *real fluids* in which the pair interactions extend beyond nearest neighbors, we expect that the general form of the map will involve an Ising Hamiltonian of the form

$$\mathcal{H}_I = \sum_i H_I(\{K\}, H) s_i + \frac{1}{2} \sum_{i \neq j} K_I(|i-j|; \{K\}, H) s_i s_j, \quad (12)$$

where $K_I(|i-j|)$ is the general spin-spin coupling constant. Proceeding as before to calculate the magnetization conjugate to H , we see immediately that the energylike term involved is

$$\frac{1}{N} \frac{1}{2} \sum_{i \neq j} \frac{\partial K_I(|i-j|; \{K\}, H)}{\partial H} \langle s_i s_j \rangle_I. \quad (13)$$

In drawing the analogy with the fluid case to be discussed later, we suggest that the generalization of Eq. (13) to a continuum system will involve the integral of a chemical-potential-dependent effective pair potential

$$\int d^3r \rho^{(2)}(r) \frac{\partial \phi(r; \mu, T)}{\partial \mu}, \quad (14)$$

where $\rho^{(2)}$ is the two-body distribution function.

The concept of thermodynamic-state-dependent potentials appears quite naturally in a variety of contexts; obvious examples include theories of electrolyte screening, the structural and electronic properties of metals, and the tracing out of angular variables to define a spherically symmetric effective intermolecular potential.³⁰ An important point to emphasize in applying this notion to systems near second-order phase transitions is that the effective potentials involved are most clearly defined in the *grand canonical ensemble*, where they are then viewed fundamentally as functions of the thermodynamic fields.³⁰ In the canonical ensemble they are functions of the conjugate densities. This distinction is important in the critical region since the densities themselves may develop singular behavior, implying potentials which would then be singular as well. This can be shown to imply thermodynamic inconsistencies. As emphasized in other contexts,^{31,32} the theory of critical phenomena is most naturally cast in terms of the governing thermodynamic fields, which take on common values in coexisting phases.

III. THREE-BODY INTERACTIONS IN FLUIDS

A. van der Waals theory

In any classical theory of the liquid-vapor transition of a one-component fluid, the expansion for the pressure near the critical point, in units of the critical pressure P_c , takes the form³³

$$\frac{P}{P_c} = \sum_{m,n} \frac{1}{m!} \frac{1}{n!} P_{mn} (\Delta\rho)^m (\Delta T)^n, \quad (15)$$

where the deviation of the number density $\rho = N/V$ from ρ_c , its value at the critical point, is $\Delta\rho = (\rho - \rho_c)/\rho_c$, and $\Delta T = (T - T_c)/T_c$. Both the Helmholtz free energy and the chemical potential possess analogous expansions, with coefficients F_{mn} and μ_{mn} . From the usual Maxwell construction, one finds that the densities in the two branches of the coexistence curve differ from the critical density with the following asymptotic form:

$$(\Delta\rho)_{l,v} = \pm A\beta t^\beta + A_1 t + \dots, \quad (16)$$

where $t = -\Delta T$, $\beta = \frac{1}{2}$ in this mean-field theory, $A\beta = (6P_{11}/P_{30})^{1/2}$, and the slope of the diameter is³³

$$A_1 = \frac{P_{21}}{P_{30}} - \frac{3}{5} \frac{P_{11}P_{40}}{P_{30}^2} + \frac{4}{5} \frac{P_{11}}{P_{30}}. \quad (17)$$

For the van der Waals equation of state, in which the free energy is

$$F = Nk_B T \ln \left[\frac{N\Lambda^3}{e(V-Nb)} \right] - aN \left[\frac{N}{V} \right], \quad (18)$$

with Λ the thermal wavelength, A_1 has the universal value of $\frac{2}{5}$.

To include three-body interactions at the level of mean-field theory, we supplement the free energy in Eq. (18) with the term

$$F_3 = qN \left[\frac{N}{V} \right]^2, \quad (19)$$

where q is the integrated strength of the three-body potential ψ ,

$$q = \frac{1}{6} \int \int d^3r d^3r' \psi(\mathbf{r}, \mathbf{r}', \mathbf{r} - \mathbf{r}') g_{\text{HS}}^{(3)}(\mathbf{r}, \mathbf{r}', \mathbf{r} - \mathbf{r}'). \quad (20)$$

with $g_{\text{HS}}^{(3)}$ the hard-sphere three-body distribution function. This is the direct analog of the microscopic definition³⁴ of the attractive parameter a in the simple van der Waals equation (18),

$$a = -\frac{1}{2} \int d^3r \phi(r) g_{\text{HS}}^{(2)}(r), \quad (21)$$

where $g_{\text{HS}}^{(2)}(r)$ is the hard-sphere radial distribution function, taken to be a step function at the hard-core diameter σ .

In the presence of the triplet interactions, it is still possible to express the critical parameters in closed form, and we write them in terms of the values which pertain when $q=0$, namely,

$$\rho_c = \frac{1}{3b} \bar{\rho}(x), \quad (22)$$

$$k_B T_c = \frac{8a}{27b} \tilde{T}(x), \quad (23)$$

$$P_c = \frac{a}{27b^2} \bar{P}(x), \quad (24)$$

where

$$\bar{\rho}(x) = \frac{3}{4} + \frac{3}{8x} \left[1 - \left[1 - \frac{4x}{3} + 4x^2 \right]^{1/2} \right], \quad (25)$$

$$\tilde{T}(x) = \frac{9}{4} \bar{\rho}(x) [1 - x \bar{\rho}(x)] [1 - \frac{1}{3} \bar{\rho}(x)]^2, \quad (26)$$

and

$$\bar{P}(x) = \frac{8}{3} \frac{\tilde{T}(x) \bar{\rho}(x)}{1 - \frac{1}{3} \bar{\rho}(x)} - 3\bar{\rho}^2(x) + 2x\bar{\rho}^3(x). \quad (27)$$

The thermodynamic properties of the system *all* depend *explicitly* on the dimensionless parameter

$$x \equiv q/ab, \quad (28)$$

which, in mean-field theory, is simply the ratio of three-

body to two-body potentials. Since $q \sim \alpha_p^3$, $a \sim \alpha_p^2$, and the critical density is proportional to b^{-1} , x is indeed proportional to the product of the polarizability and the critical number density, $\alpha_p \rho_c$, to leading order in the three-body interaction. For the systems of interest here, we need only consider the small- x expansions of the various thermodynamic quantities: (a) the order parameter amplitude,

$$A_\beta = 2 + \frac{2}{3}x + \dots; \quad (29)$$

(b) diameter slope,

$$A_1 = \frac{2}{5} + \frac{22}{15}x + \dots; \quad (30)$$

(c) critical compressibility factor,

$$Z_c \equiv \frac{P_c}{\rho_c k_B T_c} = \frac{3}{8} - \frac{1}{8}x + \dots. \quad (31)$$

The constant of proportionality between the parameter x and the product $\alpha_p \rho_c$ is given in terms of the integrals in Eqs. (20) and (21) which are very sensitive to the short-range structure of the two- and three-body correlations and of the potentials themselves, which certainly acquire strong repulsive components at small distances. Rather than approach this complex question numerically, we may note instead that the van der Waals theory predicts relationships between the dependence of various quantities on x which are independent of the constant of proportionality. For example, from Eqs. (29) to (31), we find that the slope of the A_1 versus $\alpha_p \rho_c$ and Z_c versus $\alpha_p \rho_c$ curves are related by a pure number:

$$\frac{dA_1}{d\alpha_p \rho_c} \bigg/ \frac{dZ_c}{d\alpha_p \rho_c} = -\frac{176}{15} + O(x) \approx -11.73. \dots \quad (32)$$

While the precise numerical value of this ratio is expected to be model dependent, its significance lies in both its *magnitude* (of order 10) and its *sign*, for the fact that the diameter slope *increases* with positive values of the parameter x is in accord with expectations for the Axilrod-Teller potential, which is repulsive for the majority of the orientational phase space available to the triad of particles.

It is also predicted that the order-parameter amplitude increases in parallel with the diameter slope. To leading order in x , we find

$$A_\beta = \frac{20}{11} + \frac{5}{11} A_1, \quad (33)$$

the slope of which ($\frac{5}{11}$), obtained *with no adjustable parameters*, is shown in Sec. IV to be in remarkable quantitative agreement with the data for those same fluids.

B. Perturbation theory for fluids

We next present a simple derivation of an effective pair potential which accounts for the presence of three-body interactions in fluids, and which by its explicit fugacity dependence leads to thermodynamic field mixing and a singular diameter. The development of this effective two-body potential proceeds from the enforced equality of a thermodynamic quantity in a fluid with three-body forces with the same quantity in a system governed solely by an effective pair potential. As has been shown by Casanova

et al.,³⁵ different effective potentials arise from considering different thermodynamic quantities, such as the pair correlation function and the pressure. In keeping with the discussion above, in which we emphasized the importance of framing the smoothness postulate in terms of thermodynamic *fields*, rather than their conjugate densities, we find it most natural to determine the effective potential in a way that preserves the grand canonical partition function $\Xi(T, \mu, V)$, or, equivalently, the thermodynamic potential $\Omega = -k_B T \ln \Xi$.

The interaction Hamiltonian of the fluid is assumed to be a sum of two-body potentials ϕ and triplet potentials ψ :

$$\mathcal{H} = \frac{1}{2!} \sum_{i \neq j} \phi_{ij} + \frac{1}{3!} \sum_{i \neq j \neq k} \psi_{ijk}. \quad (34)$$

In seeking an effective potential $\tilde{\phi}_{ij}(r_{ij}; T, \mu)$ which preserves the thermodynamic potential, we may, for instance, keep the fugacity $z = \exp(\mu/k_B T)$ fixed and vary only the potential, writing

$$-k_B T \ln \Xi(z, \phi, \psi) = -k_B T \ln \Xi(z, \tilde{\phi}, 0). \quad (35)$$

Alternatively, ϕ may be fixed and only z varied, or yet again both ϕ and z can be adjusted. If we impose only the single constraint that the free energy be preserved, there is no *a priori* reason to prefer one formulation over any other. We discuss in detail elsewhere²⁸ a transformation which is unique for *lattice* models, and shall discuss here an approach based on Eq. (35), for it is not only conceptually the simplest, but it also allows us to make contact with the results obtained previously in the canonical ensemble.³⁵

The leading order term in a functional Taylor expansion of the right-hand side of Eq. (35) is

$$\begin{aligned} \Omega(z, \tilde{\phi}, 0) &= \Omega(z, \phi, 0) \\ &+ \int \int d\mathbf{r}_1 d\mathbf{r}_2 \frac{\delta \Omega(z, \phi, 0)}{\delta \phi(\mathbf{r}_1, \mathbf{r}_2)} \\ &\quad \times [\tilde{\phi}(\mathbf{r}_1, \mathbf{r}_2) - \phi(\mathbf{r}_1, \mathbf{r}_2)] + \dots \end{aligned} \quad (36)$$

Denoting with a subscript 0 quantities pertaining to the “reference” system (that with only the pair potential ϕ), we have

$$\frac{\delta \Omega(z, \phi, 0)}{\delta \phi(\mathbf{r}_1, \mathbf{r}_2)} = \frac{1}{2!} \rho_0^{(2)}(\mathbf{r}_1, \mathbf{r}_2), \quad (37)$$

where $\rho_0^{(2)}$ is the reference two-point distribution function. On the other hand, ψ may be treated as a perturbation on the left-hand side of Eq. (35), with the first-order perturbation theory result

$$\begin{aligned} \Omega(z, \phi, \psi) &= \Omega(z, \phi, 0) \\ &+ \frac{1}{3!} \int \int \int d\mathbf{r}_1 d\mathbf{r}_2 d\mathbf{r}_3 \rho_0^{(3)} \\ &\quad \times (\mathbf{r}_1, \mathbf{r}_2, \mathbf{r}_3) \psi(\mathbf{r}_1, \mathbf{r}_2, \mathbf{r}_3) + \dots \end{aligned} \quad (38)$$

with $\rho_0^{(3)}$ the three-body distribution function of the reference system. Equating Eqs. (36) and (38), and using (37), we find to first order

$$\int \int d\mathbf{r}_1 d\mathbf{r}_2 \left\{ \frac{1}{2!} \rho_0^{(2)}(\mathbf{r}_1, \mathbf{r}_2) [\tilde{\phi}(\mathbf{r}_1, \mathbf{r}_2) - \phi(\mathbf{r}_1, \mathbf{r}_2)] - \frac{1}{3!} \int d\mathbf{r}_3 \rho_0^{(3)}(\mathbf{r}_1, \mathbf{r}_2, \mathbf{r}_3) \psi(\mathbf{r}_1, \mathbf{r}_2, \mathbf{r}_3) \right\} = 0. \quad (39)$$

In this form, it is clear that there is an infinity of choices for the function $\tilde{\phi}$ which will satisfy Eq. (39), for $\tilde{\phi}$ is only defined to within a function whose integral with the two-body distribution function vanishes. The choice for $\tilde{\phi}$ that is least arbitrary and the one for which previous results are recovered is the one for which the integrand in large parentheses is identically zero. Following Rowlinson,³⁰ the effective potential is defined in the *low-fugacity limit* as a trace over all degrees of freedom which are to be eliminated (here, the presence of a third particle). We thus invoke the fundamental relations

$$\Xi_0 \rho_0^{(2)}(\mathbf{r}_1, \mathbf{r}_2) = z^2 \exp[-\phi(\mathbf{r}_{12})/k_B T] + O(z^3) \quad (40)$$

and

$$\Xi_0 \rho_0^{(3)}(\mathbf{r}_1, \mathbf{r}_2, \mathbf{r}_3) = z^3 \exp\{-[\phi(\mathbf{r}_{12}) + \phi(\mathbf{r}_{13}) + \phi(\mathbf{r}_{23})]/k_B T\} + O(z^4). \quad (41)$$

The effective potential is thus

$$\tilde{\phi}(\mathbf{r}_{12}) = \phi(\mathbf{r}_{12}) + \frac{1}{3} z \int d\mathbf{r}_3 \exp\{-[\phi(\mathbf{r}_{13}) + \phi(\mathbf{r}_{23})]/k_B T\} \times \psi(\mathbf{r}_{12}, \mathbf{r}_{13}, \mathbf{r}_{23}). \quad (42)$$

This leading contribution to $\tilde{\phi}$ is related to the form obtained by Casanova *et al.* from diagrammatic analyses of the pair correlation function and of the pressure, as represented by its virial expansion. Their result is that if $\tilde{f}_{12} = \exp(-\tilde{\phi}_{12}/k_B T) - 1$ is the effective Mayer f function desired at density ρ , it is related to the bare $f_{12} = \exp(-\phi_{12}/k_B T) - 1$ by

$$\tilde{f}_{12} = f_{12} + (f_{12} + 1) \left[c\rho \int d\mathbf{r}_3 e_{13} e_{23} f_{123} + O(\rho^2) \right], \quad (43)$$

with $f_{123} = \exp(-\psi_{123}/k_B T) - 1$, and $e_{ij} = f_{ij} + 1$. The numerical factor c depends on the thermodynamic property under consideration, and is unity for the pair correlation function, and $\frac{1}{3}$ for the pressure. Linearization of Eq. (43) for $(\tilde{\phi} - \phi)/k_B T$ and $\psi/k_B T$ small gives the leading order term in Eq. (42), provided the low-density correspondence $z \rightarrow \rho$ is used. These results also agree in form with those of Sinanoğlu,³⁶ who determined the effective potential by equating the internal energy of the fluid with triplet potentials and that with the effective pair potential, and of Rushbrooke and Silbert,³⁷ in the context of the hypernetted-chain equation. It can be shown³⁵ that at long range this effective potential decays as r^{-6} , as does the bare potential, and therefore does not affect the universality class of the fluid.

It is instructive to consider a graphical representation of Eq. (42), as shown in Fig. 2(c), for it emphasizes the similarity between the decorated-lattice transformation and the perturbation theory just outlined. In both cases, the effective pair interaction is arrived at by a statistical trace over an intervening particle. Since the magnitude of the effect of that third particle depends on the probability that

it is present, the effective potential must depend on the one-body field to which that density is conjugate, namely, the chemical potential. This tracing out of "intervening" particles is also analogous to the way in which thermodynamic field mixing enters into the penetrable-sphere models⁷ and to the screening action of the electron gas in metals.¹⁸

With this effective potential, we may demonstrate the existence of a singular diameter by considering the thermodynamic potential of a fluid with general z - and T -dependent interactions and effective fugacity. Let $\omega_0(z, \phi)$ be the grand free energy per unit volume of a fluid with only pairwise interactions, and $\tilde{\omega} = \omega_0[\tilde{z}(z, T), \tilde{\phi}(z, T)] + \omega_b(z, T)$ be the free energy of the three-body fluid under the approximate map, with ω_b an analytic background contribution. The thermodynamic density is

$$\begin{aligned} \tilde{\rho} &= - \frac{\partial \ln \tilde{\omega}}{\partial \ln z} \\ &= - \frac{z}{k_B T} \frac{\partial \omega_b}{\partial z} - \frac{z}{\tilde{z}} \frac{\partial \tilde{z}}{\partial z} \rho_0^{(1)}(\tilde{z}, \tilde{\phi}) \\ &\quad - \frac{1}{2} \frac{z}{k_B T} \int d\mathbf{r} \rho_0^{(2)}(\mathbf{r}) \frac{\partial \tilde{\phi}(\mathbf{r})}{\partial z}, \end{aligned} \quad (44)$$

where $\rho^{(n)} = \langle \hat{\rho}^{(n)} \rangle$ is the ensemble average of the n -body density operator. The energylike singularity in the density then arises, as discussed before, from the temperature dependence of the short-range behavior of the two-body distribution function. It should be remarked that this is the same mechanism governing the singular behavior both of the resistivity of a ferromagnet at its Curie point,³⁸ and of the dielectric constant of a fluid at its liquid-vapor critical point.³⁹ Through Eq. (42) and the observation that T_c scales with the strength of the pair potential, the amplitude of the energy singularity is seen to be proportional to the relative strength of the triplet to pair interactions, and hence to the critical polarizability product $\alpha_\rho \rho_c$.

IV. EXPERIMENTAL RESULTS

In this section we present an analysis of measurements of the coexistence-curve diameters of Ne, N₂, C₂H₄, C₂H₆, and SF₆. We first review briefly the methods used to obtain data; more detailed descriptions have appeared previously.^{14,20-22}

Density data on HD, Ne, and N₂ were obtained from the capacitors formed by five coin-shaped parallel electrodes stacked on top of one another. Values of the dielectric constant determined in these capacitors were converted to mass densities with the Clausius-Mossotti relation. The diameters of HD, Ne, and N₂ were determined from the vapor density at the top capacitor and the liquid density at the bottom gap which were separated by 0.64 cm, with a gap width of 0.0076 cm. Density differences at various heights were used previously²⁰ to

determine the shape of the coexistence curve (i.e., the order parameter), the compressibility in the one- and two-phase regions, and the density as a function of chemical potential near T_c . The critical exponents β and γ , describing the behavior of the order parameter and compressibility as $t \rightarrow 0$, were found in that experiment to be 0.327 ± 0.002 and 1.24 ± 0.01 , respectively, both in excellent agreement with theoretical predictions. It also proved possible to make a fairly precise determination of the corrections-to-scaling exponent Δ , of 0.50 ± 0.03 , also in good agreement with theory. The critical temperatures of Ne and N_2 , determined as free parameters in a non-linear least-squares analysis of the data along different thermodynamic paths, are shown in Table I. The uncertainties in the reported values, reflecting the spread among the different determinations, are 0.0005 K (HD), 0.0003 K (Ne), and 0.0002 K (N_2). The quoted critical temperatures are relative to an absolute temperature scale, accurate to 25 mK. These previously determined values of β , γ , Δ , and T_c are used in the present analysis of the diameter, and with the exponent relation $\alpha = 2 - 2\beta - \gamma$, they yield $\alpha = 0.11$. The data on the coexistence curve of HD is available only over a limited temperature range, and is used in this paper only to obtain the slope of the diameter outside the asymptotic critical region.

Density data on C_2H_4 and C_2H_6 were obtained from measurements of the refractive index using a prism-shaped sample cell. The index data were converted to densities using values of the Lorenz-Lorentz coefficient measured with the same apparatus.^{21,22} In both cases the critical temperature was determined for the present analysis from a fit of the form

$$\frac{\rho_l - \rho_v}{2\rho_c} = A_\beta t^\beta + A_{\beta+\Delta} t^{\beta+\Delta} + A_{\beta+2\Delta} t^{\beta+2\Delta}, \quad (45)$$

with β fixed at 0.327 and Δ at 0.5. The critical temperature thus determined for C_2H_6 is slightly different from that published previously.²² A complete account of the C_2H_4 order-parameter measurements will be published elsewhere.²¹

We have also examined the data of Weiner, Langley, and Ford¹⁴ on SF_6 , obtained also from dielectric-constant measurements. We use the critical temperature as reported in the thesis of Weiner.¹⁴ These data, which have also been analyzed by Ley-Koo and Green,¹⁵ and by Nicoll and Albright¹⁰ are here reanalyzed over identical temperature ranges and with the same functional forms as used for Ne, N_2 , C_2H_4 , and C_2H_6 , allowing for a consistent comparison of the various fluids.

The diameters of Ne, N_2 , C_2H_4 , C_2H_6 , and SF_6 are shown in Fig. 3, and it is clear that for $t \leq 3 \times 10^{-3}$ all show negative deviations from the linear behavior which holds at larger t , indicated by the dashed lines (see below), and that those deviations increase systematically with the critical temperature (and therefore the polarizability) of the system.

Before interpreting the results on the diameter anomaly as possible evidence of a singular term representing field mixing, it is reasonable to consider other possible mechanisms which may give rise to such a negative deviation. Although those deviations could, in principle, reflect the

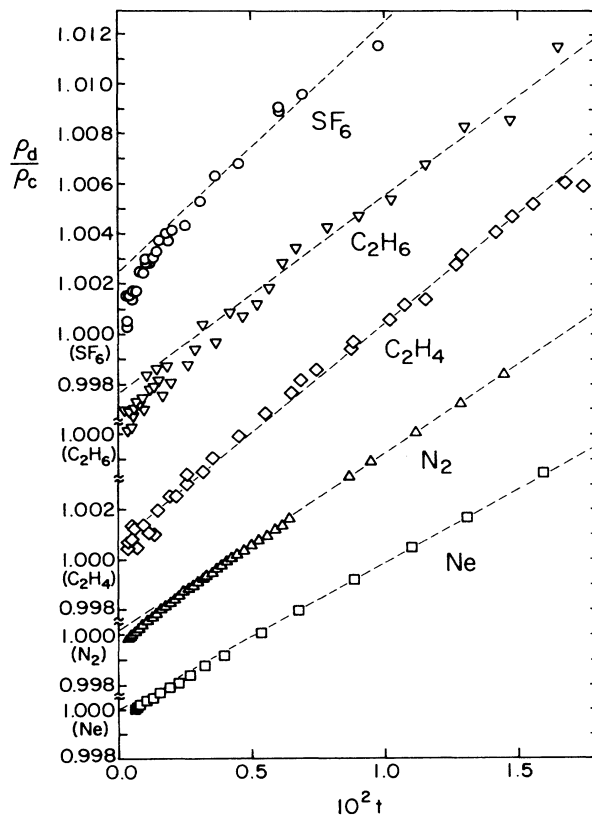


FIG. 3. Coexistence-curve diameters as functions of reduced temperature for Ne, N_2 , C_2H_4 , C_2H_6 , and SF_6 . Dashed lines indicate linear fits to the data far from the critical point.

presence of a weak critical anomaly in the dielectric constant ϵ or index of refraction,³⁹ this appears unlikely to be the case here: It has been shown^{40,41} for both Ne and SF_6 that if there is an anomaly in the dielectric constant, its magnitude is less than 5 parts in 10^6 near $t \approx 10^{-4}$. In the case of CO, a polar fluid, a small increase in ϵ ,⁴⁰ on the order of 0.1%, is seen at a reduced temperature of 10^{-4} above T_c .

Another important effect to be considered is the possible formation of wetting layers that intrude between the solid surfaces and the bulk vapor phase.^{42,43} For SF_6 near its critical temperature, these layers have been found⁴³ to be on the order of 200 Å thick. With a capacitor gap of 0.0076 cm as in the experiments HD, Ne, and N_2 , and with allowance for the temperature-dependent density difference between liquid and vapor, we estimate that the presence of such films on both faces of the gap should contribute a deviation on the order of 0.005%, in the temperature range $t \sim 5 \times 10^{-4} - 1 \times 10^{-2}$. An effect of this magnitude is at least a factor of 10 smaller than the observed deviations in Ne and N_2 . Such an effect on the SF_6 results should be even smaller, since the capacitor gap there was 0.02 cm. It is significant that the observed diameter deviation for ethane, as determined through index of refraction measurements, is on the same order as that for Ne, N_2 , and SF_6 , for this suggests that intruding wetting layers, if they exist at all, are not important, given that the surface to volume ratio in these experiments are

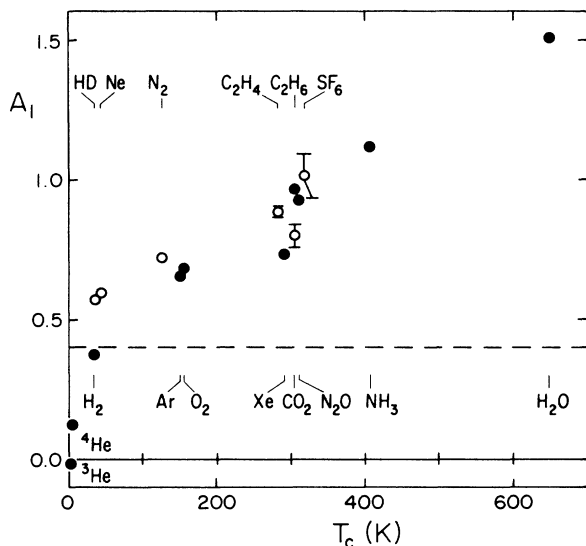


FIG. 4. Slope of diameter in outer temperature range vs critical temperature. Data are from Ref. 6 (solid circles) and present work (open circles). The dashed line at $A_1 = \frac{2}{5}$ is the universal prediction of the van der Waals equation of state for a system governed by pairwise-additive interactions.

263 cm^{-1} (Ne, N_2), 100 cm^{-1} (SF_6), and 4 cm^{-1} (C_2H_6).

It has long been known⁴⁴ that an incorrect choice of order parameter can introduce a spurious nonanalyticity into the diameter which carries an exponent of $2\beta \approx 0.65$. Although there are no rigorous arguments which require that the number density be the correct order parameter for a fluid, this quantity is usually considered the appropriate choice, in that it is conjugate to the one-body operator, the chemical potential, just as the magnetization of a ferromagnet is conjugate to the external magnetic field. In the analysis below, the high-precision data on Ne and N_2 appear to favor a $1-\alpha$ singularity as the dominant nonanalyticity. In the recent determination of the coexistence curves of cesium and rubidium,¹⁷ it was found that density is clearly preferred over specific volume as the order parameter.

The measured diameters as a function of temperature, over the range $3 \times 10^{-4} < t < 2 \times 10^{-2}$ are listed in Tables II–VII. With the exception of HD, for which the data is limited, all analyses discussed below were performed on the data in the full temperature range, which is further divided into what we term the *inner* ($3 \times 10^{-4} < t < 2 \times 10^{-3}$) and *outer* ($8 \times 10^{-3} < t < 2 \times 10^{-2}$) regions; the particular ranges for each fluid are given in the captions to Tables VIII–XII, which contain the results of linear least-squares fits to a variety of functional forms over the various ranges. Quoted uncertainties represent one standard deviation.

The first analysis we discuss is that of the data in the outer region which is fit by the form

$$\rho_d = A_0 + A_1 t. \quad (46)$$

We find that the value of A_1 , shown in the first line of the Tables, increases systematically with the critical tempera-

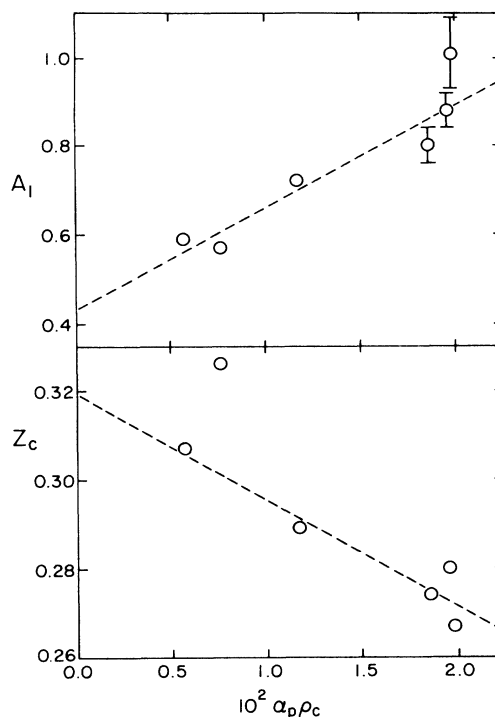


FIG. 5. Diameter slope A_1 and compressibility factor Z_c vs critical polarizability product. Dashed lines are the fitted linear relations, with the omission of the compressibility factor of HD, as described in text.

ture, as has been noted before.⁴⁵ Figure 4 shows this data, along with that of other fluids as reported in the literature.⁶ It is these linear fits which are shown as the dashed lines in Fig. 3. Remarkably, as the critical temperature decreases, the slope of the diameter in the outer range approaches closely the van der Waals value of $\frac{2}{5}$ (with the exception of the helium isotopes; see below), and there is also clearly a trend toward higher slopes with increasing T_c , in accord with the discussion of three-body effects in Sec. III. There, we suggested that the slope should be a linear function of the dimensionless polarizability factor $\alpha_p \rho_c$, and a test of this is shown in Fig. 5(a). The relation appears to be borne out by the data, with the dashed line a weighted least-squares fit of a linear form. We find

$$A_1 = (0.43 \pm 0.04) + (23.0 \pm 4.6) \alpha_p \rho_c. \quad (47)$$

The variation of the compressibility factor with $\alpha_p \rho_c$ is shown in Fig. 5(b), and with the exception of HD, a good linear relationship is found. The deviation of HD from the trend common to the remaining systems is very likely to be a quantum-mechanical effect, for as the thermal de Broglie wavelength increases, so too does the apparent size of the particles, which will increase the pressure and lower the number density, thus raising the compressibility factor. Indeed, a comparison⁴⁶ of the compressibility factors for the isoelectronic series H_2 , HD, HT, D_2 , DT, and T_2 does show a general trend toward higher values of Z_c with an increase in the de Boer parameter

TABLE II. Coexistence curve of HD.

t	ρ_v/ρ_c	ρ_l/ρ_c
0.005 864	0.745 230 1	1.266 562 9
0.005 872	0.745 158 6	1.266 591 7
0.005 285	0.754 387 8	1.256 683 3
0.004 943	0.760 144 0	1.250 600 3
0.004 602	0.766 106 3	1.244 271 9
0.004 261	0.772 406 4	1.237 659 0
0.003 926	0.778 889 8	1.230 807 2
0.003 695	0.783 513 2	1.225 838 7
0.003 479	0.788 114 7	1.221 072 0
0.003 252	0.793 065 4	1.215 863 3
0.003 025	0.798 198 1	1.210 485 8
0.002 799	0.803 608 8	1.204 809 5
0.002 568	0.809 405 9	1.198 754 6
0.002 350	0.815 266 4	1.192 684 7
0.002 125	0.821 682 2	1.186 045 5
0.001 904	0.828 402 3	1.178 978 9
0.001 676	0.835 944 0	1.171 435 6
0.001 448	0.843 948 4	1.162 856 4
0.001 228	0.852 717 5	1.153 928 6
0.001 007	0.862 494 3	1.143 948 4
0.000 892	0.868 181 8	1.138 165 1
0.000 777	0.874 234 6	1.131 919 5
0.000 663	0.880 930 8	1.125 030 3
0.000 549	0.888 380 5	1.117 461 9
0.000 435	0.896 948 1	1.108 788 6
0.000 377	0.901 748 7	1.103 970 5
0.000 319	0.907 084 3	1.098 479 3
0.000 262	0.912 640 8	1.092 347 7
0.000 212	0.918 685 1	1.086 610 6
0.000 157	0.926 200 3	1.079 013 4
0.000 104	0.935 396 3	1.069 826 2

TABLE III. Coexistence curve of Ne.

t	ρ_v/ρ_c	ρ_l/ρ_c
0.022 402	0.552 318 7	1.473 898 1
0.018 793	0.578 444 5	1.443 735 9
0.015 949	0.601 674 8	1.417 193 1
0.013 110	0.627 734 0	1.387 593 0
0.010 983	0.649 887 0	1.362 973 0
0.008 865	0.675 004 5	1.335 398 4
0.006 754	0.704 303 3	1.303 536 7
0.005 342	0.727 395 9	1.278 725 7
0.003 939	0.754 694 6	1.249 688 0
0.003 240	0.770 719 5	1.232 781 0
0.002 678	0.785 243 3	1.217 489 9
0.002 259	0.797 428 3	1.204 761 4
0.001 907	0.808 855 0	1.192 888 2
0.001 558	0.821 632 7	1.179 731 3
0.001 313	0.831 702 6	1.169 269 2
0.001 070	0.842 959 8	1.157 701 6
0.000 825	0.856 260 4	1.144 181 6
0.000 722	0.862 546 0	1.137 622 2
0.000 650	0.867 175 9	1.132 866 5

$\lambda_D = h/\sigma\sqrt{m\epsilon}$, with σ the hard-core diameter, m the mass, and ϵ the pair-potential well depth. The increase in Z_c from that of T_2 ($\lambda_D \approx 1.00$) to that of H_2 ($\lambda_D \approx 1.73$) is on the order of 0.015, which is nearly the amount by which the compressibility factor of HD lies above the linear relation obeyed by the other systems. This suggests that the quantum-mechanical corrections to the equation of state are the cause of the observed deviation.

A least-squares fit to the compressibility factor data for the systems other than HD gives the relation

TABLE IV. Coexistence curve of N_2 .

t	ρ_v/ρ_c	ρ_l/ρ_c	t	ρ_v/ρ_c	ρ_l/ρ_c
0.017 795	0.572 898 9	1.452 867 4	0.003 195	0.762 097 2	1.242 190 3
0.016 154	0.586 663 6	1.436 753 7	0.003 025	0.766 538 4	1.237 600 1
0.014 504	0.601 351 7	1.419 430 2	0.002 855	0.771 091 0	1.232 751 1
0.012 850	0.617 457 6	1.401 061 6	0.002 684	0.775 863 9	1.227 711 2
0.011 184	0.635 163 8	1.381 041 9	0.002 513	0.780 799 1	1.222 493 0
0.009 511	0.654 802 7	1.358 994 3	0.002 343	0.785 972 1	1.217 044 7
0.008 670	0.665 592 4	1.347 126 2	0.002 171	0.791 475 5	1.211 319 9
0.006 416	0.698 185 9	1.311 108 9	0.002 001	0.797 167 9	1.205 352 7
0.006 137	0.702 641 1	1.306 017 2	0.001 830	0.803 183 9	1.199 030 8
0.005 857	0.707 429 6	1.300 950 8	0.001 660	0.809 625 0	1.192 340 0
0.005 575	0.712 263 1	1.295 571 5	0.001 489	0.816 442 1	1.185 150 7
0.005 292	0.717 431 0	1.290 132 2	0.001 317	0.823 888 7	1.177 479 8
0.005 008	0.722 677 6	1.284 429 1	0.001 143	0.832 051 1	1.169 066 3
0.004 727	0.728 110 8	1.278 566 9	0.000 970	0.841 100 7	1.159 741 2
0.004 444	0.733 813 9	1.272 524 4	0.000 828	0.849 251 1	1.151 217 5
0.004 248	0.737 936 9	1.268 130 6	0.000 742	0.854 597 4	1.145 731 8
0.004 049	0.742 162 2	1.263 560 2	0.000 658	0.860 328 8	1.139 805 3
0.003 877	0.745 949 8	1.259 506 8	0.000 571	0.866 801 6	1.133 384 8
0.003 705	0.749 839 5	1.255 322 4	0.000 514	0.871 247 5	1.128 707 4
0.003 535	0.753 831 3	1.251 093 5	0.000 458	0.876 120 3	1.123 765 6
0.003 365	0.757 858 9	1.246 657 6	0.000 401	0.881 378 6	1.118 406 6

TABLE V. Coexistence curve of C_2H_4 .

t	ρ_v/ρ_c	ρ_l/ρ_c
0.019 560	0.538 588	1.498 026
0.018 779	0.544 812	1.491 288
0.017 478	0.554 155	1.475 681
0.016 816	0.560 366	1.469 759
0.015 584	0.571 394	1.457 100
0.014 802	0.578 724	1.448 757
0.014 202	0.585 790	1.440 401
0.012 892	0.598 476	1.425 846
0.012 727	0.599 884	1.423 688
0.011 578	0.611 991	1.408 858
0.010 770	0.622 123	1.398 343
0.010 222	0.628 874	1.390 250
0.008 854	0.647 982	1.369 458
0.008 759	0.647 139	1.369 735
0.007 461	0.667 063	1.348 114
0.006 881	0.675 748	1.338 665
0.006 489	0.682 472	1.330 822
0.005 528	0.700 106	1.311 623
0.004 550	0.719 674	1.290 239
0.003 562	0.740 611	1.267 473
0.003 171	0.750 927	1.256 090
0.002 578	0.768 758	1.237 378
0.002 566	0.769 035	1.237 917
0.002 162	0.781 839	1.223 271
0.001 949	0.790 169	1.214 849
0.001 480	0.815 724	1.188 214
0.001 339	0.814 343	1.187 674
0.001 133	0.825 160	1.177 068
0.000 926	0.837 635	1.165 093
0.000 719	0.849 544	1.151 486
0.000 614	0.858 677	1.143 577
0.000 516	0.868 915	1.133 774
0.000 509	0.866 704	1.134 866
0.000 418	0.875 271	1.126 141
0.000 355	0.882 179	1.118 772

TABLE VI. Coexistence curve of C_2H_6 .

t	ρ_v/ρ_c	ρ_l/ρ_c
0.021 42	0.524 507	1.512 569
0.019 82	0.536 834	1.498 641
0.018 17	0.549 646	1.481 316
0.016 48	0.564 496	1.466 563
0.014 74	0.578 909	1.446 084
0.012 97	0.597 787	1.426 769
0.011 62	0.612 831	1.408 667
0.010 24	0.627 972	1.390 760
0.009 063	0.643 890	1.373 483
0.007 877	0.660 245	1.356 255
0.006 668	0.679 026	1.333 883
0.006 178	0.687 518	1.326 119
0.005 686	0.695 914	1.315 733
0.005 186	0.705 377	1.304 960
0.004 687	0.715 132	1.294 235
0.004 197	0.725 759	1.283 946
0.003 679	0.737 455	1.269 970
0.003 172	0.751 092	1.257 643
0.002 917	0.757 692	1.249 102
0.002 660	0.764 680	1.240 852
0.001 988	0.786 664	1.217 509
0.001 835	0.793 167	1.212 220
0.001 677	0.798 505	1.204 601
0.001 521	0.805 396	1.198 923
0.001 418	0.809 279	1.193 245
0.001 313	0.814 423	1.189 362
0.001 210	0.819 955	1.183 733
0.001 103	0.825 536	1.179 171
0.000 999 4	0.830 626	1.171 212
0.000 925 4	0.835 291	1.167 621
0.000 811 7	0.841 891	1.160 487
0.000 707 2	0.849 413	1.153 159
0.000 607 2	0.857 129	1.144 909
0.000 549 0	0.861 448	1.139 911
0.000 498 6	0.866 107	1.134 330
0.000 444 2	0.871 445	1.130 350
0.000 393 1	0.876 007	1.124 284
0.000 338 7	0.881 200	1.119 092
0.000 313 8	0.885 325	1.116 617

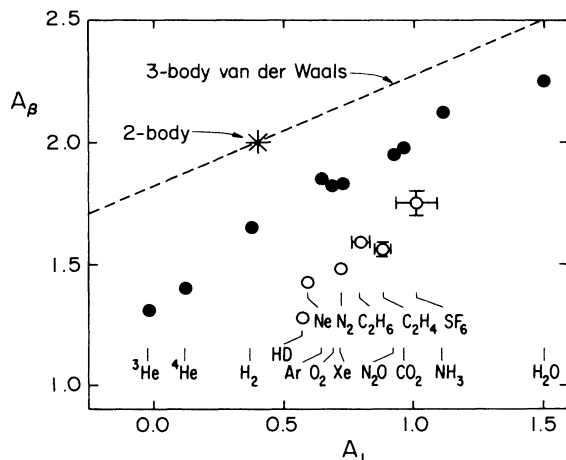


FIG. 6. Correlation of the amplitude of the order parameter (A_β) with the slope of the diameter (A_1), for a variety of fluids. The data indicated by open circles are from the present work, those with solid circles are from the sources cited in Ref. 6.

$$Z_c = (0.319 \pm 0.007) - (2.37 \pm 0.44)\alpha_p \rho_c. \quad (48)$$

The experimental value for the ratio of the two slopes in Eqs. (47) and (48) is therefore

$$\frac{dA_1}{d\alpha_p \rho_c} / \frac{dZ_c}{d\alpha_p \rho_c} = -9.7 \pm 2.6. \quad (49)$$

The measured value for this ratio is thus consistent, in both its order of magnitude and its sign, with that from the van der Waals theory presented above (≈ -11.7), lending further strong support to the notion that primarily repulsive three-body interactions are operative.

There also exists a systematic variation in the amplitude A_β with the critical temperature, like that of the diameter slope, in accord with the predictions of Eq. (29). Combining our data with previous studies of a variety of fluids, as discussed in Ref. 6, we plot in Fig. 6 the amplitude A_β

TABLE VII. Coexistence curve of SF₆, from Ref. 14.

t	ρ_v/ρ_c	ρ_l/ρ_c
0.019 052	0.530 31	1.513 80
0.018 108	0.537 26	1.503 61
0.015 453	0.560 34	1.475 43
0.012 704	0.587 00	1.442 91
0.011 060	0.607 15	1.422 40
0.009 758	0.620 20	1.402 94
0.006 912	0.661 66	1.357 62
0.006 043	0.676 87	1.340 96
0.006 012	0.677 58	1.340 62
0.004 553	0.704 73	1.308 92
0.003 668	0.726 14	1.286 54
0.003 081	0.741 83	1.268 79
0.002 557	0.756 17	1.252 52
0.002 046	0.773 90	1.234 41
0.001 920	0.778 94	1.228 54
0.001 832	0.782 42	1.225 73
0.001 541	0.794 89	1.212 60
0.001 437	0.799 89	1.206 78
0.001 324	0.804 92	1.201 14
0.001 221	0.810 28	1.195 38
0.001 183	0.811 88	1.194 13
0.001 032	0.820 62	1.185 06
0.001 023	0.820 93	1.185 01
0.001 004	0.822 26	1.182 66
0.000 922	0.826 70	1.178 28
0.000 800	0.835 17	1.169 84
0.000 706	0.841 79	1.161 67
0.000 615	0.848 75	1.154 75
0.000 511	0.857 41	1.145 21
0.000 433	0.865 67	1.13746
0.000 355	0.873 29	1.127 33
0.000 355	0.873 49	1.127 63
0.000 307	0.880 36	1.122 72

versus the diameter slope A_1 , and compare with the prediction of the van der Waals theory with three-body interactions, Eq. (33). It is clear that the experiments indicate a rather well-defined linear relationship between the two amplitudes, with a slope in good agreement with that from the van der Waals theory of $\frac{5}{11} \approx 0.45$, again supporting the hypothesis of three-body interactions in these fluids. The scatter in the data is in large part attributable to the different reduced temperature ranges over which

the various fluids were analyzed, the different values of β , and varying functional forms assumed for the coexistence curve, some including corrections to scaling, others not. It is not surprising that the actual magnitude of A_β in the mean-field theory is larger than the experimental values, since β is $\frac{1}{2}$ in the former, and nearly $\frac{1}{3}$ in the latter.

For the three-dimensional Ising model with only nearest-neighbor interactions, the value of A_β is estimated⁴⁷ to be ≈ 1.5 – 1.6 , with highly coordinated lattices such as the face-centered-cubic lattice at the low end of the range, and more open lattices like the diamond at the high end. If we imagine that this value corresponds to that of a fluid with only pair interactions, then it would serve as the fluctuation-corrected value of this amplitude for the van der Waals theory with only two-body forces. As can be seen in Fig. 6, it is roughly in agreement with the experimental data.

At first glance, it is surprising that highly polar fluids like NH₃ and H₂O follow the same trend (Fig. 6) as the nonpolar spherically symmetric systems like the rare gases, especially since the bare polarizabilities of the former are not particularly large [α_p (NH₃) = 2.26 \AA^3 , α_p (H₂O) = 1.48 \AA^3]. Yet, in the absence of any long-range dipolar correlations, it is known that the dipole-dipole potential $\phi_{dd}(r_{ij}, \omega_i, \omega_j)$, as a function of the separation r_{ij} and dipolar angles ω_i of a pair of particles, may be averaged over angles to arrive at an *effective spherically symmetric potential* $\bar{\phi}(r_{ij}, T)$. At long range, this potential decays like the ordinary dispersion energy, $\sim r^{-6}$, and thus serves simply to renormalize the amplitude of the van der Waals energy. The prescription for this *tracing out* of orientational degrees of freedom is^{46,48}

$$\exp[-\bar{\phi}(r_{ij}, T)/k_B T] = \langle \exp[-\phi_{dd}(r_{ij}, \omega_i, \omega_j)] \rangle, \quad (50)$$

where the angular statistical average of any quantity is

$$\langle \rangle \equiv \frac{1}{(4\pi)^2} \int \int d\omega_i d\omega_j \langle \rangle. \quad (51)$$

In the case of the dipole-dipole potential

$$\begin{aligned} \phi_{dd}(r_{ij}, \theta_i, \theta_j, \phi_i, \phi_j) \\ = -\frac{\mu_i \mu_j}{r_{ij}^3} [2 \cos(\theta_i) \cos(\theta_j) \\ - \sin(\theta_i) \sin(\theta_j) \cos(\phi_i - \phi_j)], \end{aligned} \quad (52)$$

TABLE VIII. Results of data analysis for Ne. Entry labeled with an asterisk includes a corrections-to-scaling term with amplitude $A_{1-\alpha+\Delta} = 0.6271 A_{1-\alpha}$. Outer range is $(0.022\ 402 > t > 0.008\ 865)$, inner range is $(0.002\ 678 > t > 0.000\ 650)$, and entire range includes all data points in Table III.

Range of t	A_0	$A_{1-\alpha}$	A_1	$A_{2\beta}$	χ^2
outer	0.999 991(74)	(0)	0.588(5)	(0)	3.122
inner	0.999 526(22)	0.357(7)	(0)	(0)	0.699
inner	0.999 637(22)	(0)	0.649(14)	(0)	0.875
inner	0.999 156(36)	(0)	(0)	0.102(2)	1.114
entire	0.999 359(33)	0.399(2)	(0)	(0)	10.37
entire	0.999 742(24)	(0)	0.604(3)	(0)	6.45
entire	0.999 575(20)	0.173(18)	0.342(27)	(0)	0.995
entire*	0.999 553(22)	0.243(25)	0.203(42)	(0)	1.012
entire	0.999 516(26)	(0)	0.527(8)	0.022(2)	1.016

TABLE IX. Results of data analysis for N_2 . Entry labeled with an asterisk includes a corrections-to-scaling term with amplitude $A_{1-\alpha+\Delta}=0.6526 A_{1-\alpha}$. Outer range is $(0.017995 > t > 0.008670)$, inner range is $(0.002513 > t > 0.000401)$, and entire range includes all data points in Table IV.

Range of t	A_0	$A_{1-\alpha}$	A_1	$A_{2\beta}$	χ^2
outer	1.000094(93)	(0)	0.716(7)	(0)	3.72
inner	0.999448(15)	0.454(5)	(0)	(0)	0.80
inner	0.999564(15)	(0)	0.840(10)	(0)	0.91
inner	0.999058(32)	(0)	(0)	0.124(2)	2.24
entire	0.999330(19)	0.480(2)	(0)	(0)	7.30
entire	0.999742(20)	(0)	0.746(3)	(0)	9.30
entire	0.999519(19)	0.259(20)	0.344(30)	(0)	1.74
entire*	0.999496(20)	0.350(25)	0.157(43)	(0)	1.64
entire	0.999449(23)	(0)	0.628(9)	0.030(2)	1.61

TABLE X. Results of data analysis for C_2H_4 . Outer range is $(0.01956 > t > 0.008759)$, inner range is $(0.001949 > t > 0.000355)$, and entire range includes all data points in Table V.

Range of t	A_0	$A_{1-\alpha}$	A_1	χ^2
outer	1.00059	(0)	0.883(37)	1.20
inner	1.00017(26)	0.517(121)	(0)	1.02
inner	1.00028(23)	(0)	0.990(226)	0.99
entire	1.00008(11)	0.579(7)	(0)	1.14
entire	1.00058(11)	(0)	0.889(11)	1.27
entire	1.00023(19)	0.401(182)	0.274(280)	1.14

TABLE XI. Results of data analysis for C_2H_6 . Outer range is $(0.021424 > t > 0.007877)$, inner range is $(0.002660 > t > 0.0003138)$, and entire range includes all data points in Table VI.

Range of t	A_0	$A_{1-\alpha}$	A_1	χ^2
outer	1.00159(55)	(0)	0.795(38)	1.58
inner	1.00013(20)	0.567(82)	(0)	1.00
inner	1.00027(19)	(0)	1.053(155)	1.03
entire	1.00017(10)	0.564(8)	(0)	1.06
entire	1.00062(11)	(0)	0.865(14)	1.44
entire	1.00010(17)	0.661(180)	-0.150(276)	1.08

TABLE XII. Results of data analysis for SF_6 . Outer range is $(0.019052 > t > 0.009758)$, inner range is $(0.002557 > t > 0.000307)$, and entire range includes all data points in Table VII.

Range of t	A_0	$A_{1-\alpha}$	A_1	χ^2
outer	1.0024(13)	(0)	1.01(8)	3.08
inner	1.00082(20)	0.801(64)	(0)	1.00
inner	1.00106(20)	(0)	1.46(13)	1.14
entire	1.00125(19)	0.690(9)	(0)	1.54
entire	1.00210(20)	(0)	1.034(16)	3.40
entire	1.00118(39)	0.754(281)	-0.096(422)	1.49

with μ_i the dipole moment on particle i , and for which $\langle \phi_{dd} \rangle = 0$, the angle-averaged potential is, to leading order in $1/k_B T$,

$$\bar{\phi}_{dd}(r, T) = -\frac{\mu^4}{3k_B T} \frac{1}{r^6}. \quad (53)$$

Similarly, the dipole-induced dipole interaction ϕ_{did} leads, through angle averaging, to an effective potential of the form

$$\bar{\phi}_{did}(r) = -\frac{2\mu^2\alpha_p}{r^6}. \quad (54)$$

Since these potentials are *attractive* and vary as r^{-6} , they may be interpreted as adding to the fluctuating-dipole potential $V_2(r) = -(3I\alpha_p^2/4)/r^6$, so that the effective polarizability is enhanced to the value $\bar{\alpha}_p$,

$$\alpha_p \rightarrow \bar{\alpha}_p = \left[\alpha_p^2 + \frac{8}{3} \frac{\mu^2\alpha_p}{I} + \frac{4}{9} \frac{\mu^4}{Ik_B T} \right]^{1/2}. \quad (55)$$

In the case of NH_3 , with $\alpha_p = 2.26 \text{ \AA}^3$, $\mu = 1.47D$, and $I = 10.2 \text{ eV}$,⁴⁸ the three terms in parentheses in Eq. (55) are, respectively, 5.11, 0.79, and 2.27 \AA^6 at the critical temperature, giving $\bar{\alpha}_p = 2.86 \text{ \AA}^3$. Thus, the induction and orientational contributions to the effective polarizability, while significant, are not dominant over the bare dispersion energy α_p^2 . With $\bar{\alpha}_p\rho_c = 0.024$, compared to $\alpha_p\rho_c = 0.019$, the experimental diameter slope A_1 and order-parameter amplitude A_β for NH_3 follow quite closely the trend obeyed by the nonpolar fluids, lending support to the notion of a dipole-enhanced effective polarizability. For H_2O , we find $\bar{\alpha}_p^2 = (2.19 + 0.67 + 2.89) \text{ \AA}^6$, or $\bar{\alpha}_p = 2.40 \text{ \AA}^3$, and it is clearly necessary to go beyond the leading-order dipolar corrections to define accurately the effective polarizability. Nevertheless, the first-order calculations give $\bar{\alpha}_p\rho_c = 0.0259$, compared with $\alpha_p\rho_c = 0.0160$, bringing the critical amplitudes as function of the critical polarizability product more nearly coincident with the trend shown by the nonpolar fluids.

The Axilrod-Teller potential is not the only important three-body contribution to the thermodynamic properties of fluids, for, as we remarked in the Introduction, three-particle exchange forces are relatively more important among the smaller, less polarizable fluids whose critical temperatures fall below $\sim 20 \text{ K}$. In particular, as we see in Fig. 4, the diameter slopes of the helium isotopes are extremely small,^{45,49} far *below* the van der Waals prediction of $A_1 = \frac{2}{5}$. Yet, they do follow well the same trend in A_β versus A_1 that all of the other fluids do, and this is suggestive of the presence of an *attractive* triplet potential, in contrast to the repulsive triple-dipole interaction which acts to *increase* the slope from the value $\frac{2}{5}$. Indeed, quantum-mechanical calculations⁵⁰ do suggest that the exchange interactions dominate the dispersion forces in helium, and are of the opposite sign. On the other hand, from the de Boer parameters of the helium isotopes, and the discussion in Sec. IV on the properties of HD, it is certain that quantum corrections to the equation of state are large. Their full effect on the thermodynamic properties in the critical region remains an open question.

We next describe the analysis of the diameter anomalies

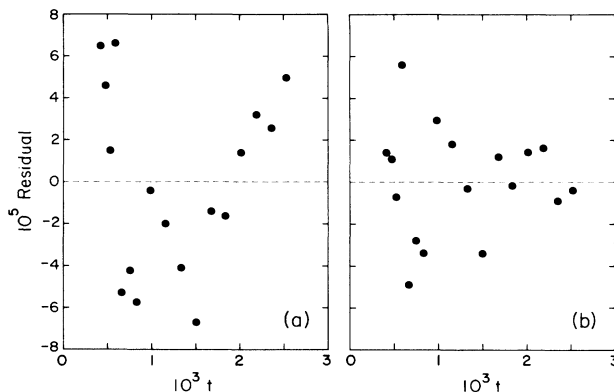


FIG. 7. Residual plots from fits of the diameter of N_2 in the inner temperature range. The fitting function is $A_0 + A_{2\beta}t^{2\beta}$ in (a), for which there is systematic variation seen in the residuals, and $A_0 + A_{1-\alpha}t^{1-\alpha}$ in (b), with no systematic trends in the deviations visible.

for the five fluids. The significantly smaller scatter present in the data on neon and nitrogen allows a more detailed analysis than for the other fluids. In no cases were more than three adjustable amplitudes used in any of the fits, there being insufficient data to make accurate determinations of any more. The critical exponent α was fixed at 0.11 in all of the least-squares fits, with only the amplitudes A as the variable parameters, entering linearly into the analysis. In the inner temperature region, the measured diameters are found to be consistent with both the functional form $A_0 + A_1t$ and $A_0 + A_{1-\alpha}t^{1-\alpha}$, the latter almost always preferred based on its χ^2 value. Evidence for the curvature of the diameter is the fact that the amplitude A_1 fit in the inner region is always larger than that obtained in the outer region. The amplitudes A_1 and $A_{1-\alpha}$ obtained in the inner-region fits also exhibit the same trend with respect to the critical temperature as exhibited by the slope in the outer region. Examination of

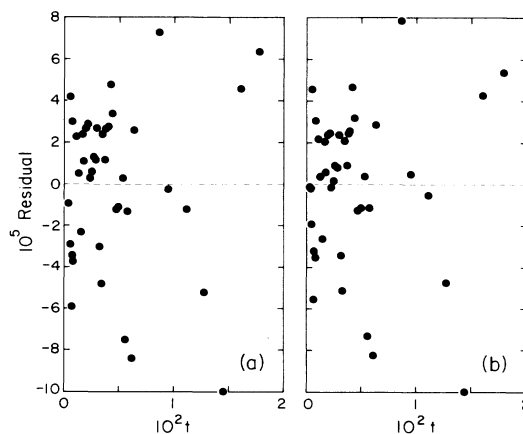


FIG. 8. Residual plots from fits of the diameter of N_2 over the entire temperature range. In (a) the diameter is taken to have the form $A_0 + A_{1-\alpha}t^{1-\alpha} + A_1t$, while in (b) a correction-to-scaling term $A_{1-\alpha+\Delta}t^{1-\alpha+\Delta}$ is added, with $A_{1-\alpha+\Delta}/A_{1-\alpha} = 0.6526$.

the extrapolations to $t=0$ of the deviations from linear diameters confirms the existence of diameter anomalies scaling with the critical polarizability product.

The residual plots for nitrogen in Fig. 8 and the χ^2 values for neon and nitrogen also show clearly that in the inner temperature region, a functional form $A_0 + A_{2\beta}t^{2\beta}$ is not consistent with the data. In contrast to the fit of the form $A_0 + A_{1-\alpha}t^{1-\alpha}$ [Fig. 7(b)], the fit with the $t^{2\beta}$ term [Fig. 7(a)] shows systematic residual variation. However, the inclusion of a linear term into the former (last entries in Tables II and III) improves the fit considerably, making it comparable to that with a $1-\alpha$ anomaly. Since 2β is not very different from $1-\alpha$, it is not surprising that the fits of these two forms are not substantially different, and we cannot definitively rule out the presence of a 2β anomaly.

Over the entire temperature range, simple fitting functions with *only* the constant and either the A_1t or the $A_{1-\alpha}t^{1-\alpha}$ terms are not by themselves sufficient. Instead, a functional form of $A_0 + A_{1-\alpha}t^{1-\alpha} + A_1t$ or $A_0 + A_{1-\alpha}t^{1-\alpha} + A_1t + A_{1-\alpha+\Delta}t^{1-\alpha+\Delta}$ is required. In the so-called extended linear model equation of state, the ratio $A_{1-\alpha+\Delta}/A_{1-\alpha}$ can be calculated via parameters obtained from the asymptotic equation of state of the fluid.⁵¹ These ratios, 0.6271 and 0.6526 for Ne and N₂, respectively, are used to reduce the number of free parameters in the fits to the data. The variations of the amplitudes A upon the addition of the linear and corrections-to-scaling terms show that it is difficult to separate the contribution of each of these terms over the limited temperature range available. For the most accurate data on Ne and N₂, however, the coefficient of the *leading* singular term, $A_{1-\alpha}$, is relatively insensitive to the inclusion of corrections-to-scaling terms, as seen in Tables VIII and IX, and this, along with the absence of systematic deviations in the residual plots, Figs. 8(a) and 8(b), strongly suggests the existence of an energylike diameter anomaly.

Finally, from the data on N₂,²⁰ which is of the highest quality, we have determined the difference between the compressibilities in the coexisting phases, a quantity which is predicted to diverge in the presence of field mixing. This difference is computed by comparison of the densities at different heights in the capacitor stack. The data clearly show that

$$\left. \frac{\partial \rho}{\partial \mu} \right|_{\text{liq}} - \left. \frac{\partial \rho}{\partial \mu} \right|_{\text{vap}} > 0, \quad (56)$$

and there is good evidence of a critical divergence, although there is severe rounding close to the critical temperature ($t \lesssim 10^{-3}$). We recall the discussion in Sec. II, in which it was pointed out that the inequality in Eq. (56) is expected to hold in the presence of diameters whose anomalies are in the direction found for the fluids studied here, that is, $\rho_c < \rho'_c$ (Fig. 1). Mulholland *et al.*⁶ found for ⁴He, Ar, and NH₃ that the amplitude of the compressibility difference increases approximately linearly with the diameter slope, and this is completely consistent with

our expectations based on the role of three-body interactions.

V. CONCLUSIONS

We have shown that a variety of observed trends in properties relevant to the liquid-vapor symmetry of pure fluids can be understood to be a consequence of relatively weak three-body dispersion forces. The slope of the coexistence-curve diameter outside the critical region, the amplitude of singular anomaly in the diameter near T_c , the critical compressibility factor, and the order-parameter amplitude all scale with the critical polarizability product $\alpha_p \rho_c$, a dimensionless measure of the relative importance of three- versus two-body interactions. In explaining the origin of the diameter anomalies, we suggest that by a suitable map in the grand canonical ensemble, triplet interactions may be accounted for with appropriate thermodynamic-state-dependent pair potentials. In the critical region, this state dependence is the analog of thermodynamic field mixing, which, in solvable lattice and continuum models, led to the original predictions of the breakdown in the law of the rectilinear diameter. The correlations other than that of the anomaly amplitude are explained semiquantitatively with a simple van der Waals model of a fluid with pair and triplet interactions. A more detailed study of the role of many-body interactions at second-order phase transitions, both from the point of view of the equilibrium theory of fluids, and with field-theoretic methods, is desirable.

Finally, having identified the critical polarizability product $\alpha_p \rho_c$ as a convenient dimensionless measure of the relative importance of three-body interactions, we pose the question of the importance of even higher-order interactions in extremely polarizable fluids. Mercury, for example, while a metal at room temperature, is thought to be a semiconductor at its critical point, and we might imagine that a large part of its cohesive energy is due to dispersion forces. With a gas-phase polarizability of $\alpha_p = 5.1 \text{ \AA}^3$ and a critical density of $\sim 5.8 \text{ g/cm}^3$, its critical polarizability product is 0.089, a factor of ≈ 4.5 larger than that of SF₆. One expects, therefore, that even four- and higher-body interactions will be important, and this should have measurable consequences in condensed phases. Indeed, preliminary evidence⁵² suggests the presence of a very large amplitude diameter anomaly near the critical point of Hg.

ACKNOWLEDGMENTS

We are grateful to M. E. Fisher and B. Widom for important insights, to P. C. Albright, J. M. H. Levelt Sengers, R. Lipowsky, A. C. Maggs, M. R. Moldover, J. F. Nicoll, A. Parola, J. J. Rehr, and G. Stell for helpful discussions, and to F. Hensel and L. Reatto for communication of results prior to publication. This work was supported in part by the National Science Foundation (NSF), through Grant Nos. DMR82-06109 and 79-27279 at Pennsylvania State University, and No. DMR84-15669 at

Cornell University, and, at the University of British Columbia, by the Natural Sciences and Engineering Research Council of Canada. The partial support of R.E.G. by the Fannie and John Hertz Foundation is

gratefully acknowledged. M.H.W.C. acknowledges the support of the Guggenheim Foundation and the hospitality of the Laboratory of Atomic and Solid State Physics at Cornell.

- *Present address: The Standard Oil Company, Research Center, 4440 Warrensville Center Road, Cleveland, OH 44128.
- ¹M. E. Fisher, *Phys. Rev.* **113**, 969 (1959).
 - ²J. C. Wheeler, *Ann. Rev. Phys. Chem.* **28**, 411 (1977).
 - ³C. A. Vause and J. S. Walker, *Phys. Lett.* **90A**, 419 (1981); J. S. Walker and R. E. Goldstein, *ibid.* **112A**, 53 (1985).
 - ⁴R. B. Griffiths, in *Critical Phenomena in Alloys, Magnets and Superconductors*, edited by R. E. Mills, E. Ascher, and A. I. Jaffe (McGraw-Hill, New York, 1971), p. 377.
 - ⁵N. D. Mermin, *Phys. Rev. Lett.* **26**, 169 (1971); **26**, 957 (1971).
 - ⁶G. W. Mulholland, J. A. Zollweg, and J. M. H. Levelt-Sengers, *J. Chem. Phys.* **62**, 2535 (1975).
 - ⁷B. Widom and J. S. Rowlinson, *J. Chem. Phys.* **52**, 1670 (1970); J. S. Rowlinson, *Adv. Chem. Phys.* **41**, 1 (1980); P. C. Hemmer and G. Stell, *Phys. Rev. Lett.* **24**, 1284 (1970).
 - ⁸J. J. Rehr and N. D. Mermin, *Phys. Rev. A* **8**, 472 (1973).
 - ⁹N. D. Mermin and J. J. Rehr, *Phys. Rev. A* **4**, 2408 (1971).
 - ¹⁰J. F. Nicoll, *Phys. Rev. A* **24**, 2203 (1981); J. F. Nicoll and R. K. P. Zia, *Phys. Rev. B* **23**, 6157 (1981); J. F. Nicoll and P. C. Albright, in *Proceedings of the Eighth Symposium on Thermophysical Properties*, edited by J. V. Sengers (American Society of Mechanical Engineers, New York, 1982), Vol. I, p. 377.
 - ¹¹L. Cailletet and E. Matthias, *C.R. Acad. Sci.* **102**, 1202 (1886); **104**, 1563 (1887).
 - ¹²J. M. H. Levelt-Sengers, *Physica (Utrecht)* **73**, 73 (1974); J. S. Rowlinson, *Nature (London)* **244**, 414 (1973); J. V. Sengers and J. M. H. Levelt-Sengers, in *Progress in Liquid Physics*, edited by C. A. Croxton (Wiley, Chichester, England, 1978); S. C. Greer and M. R. Moldover, *Ann. Rev. Phys. Chem.* **32**, 233 (1981).
 - ¹³S. C. Greer, B. K. Das, A. Kumar, and E. S. R. Gopal, *J. Chem. Phys.* **79**, 4545 (1983), and references therein. For very recent work suggesting the presence of a singular diameter in binary mixtures, see V. Vani, S. Guha, and E. S. R. Gopal, *ibid.* **84**, 3999 (1986).
 - ¹⁴J. Weiner, K. H. Langley, and N. C. Ford, Jr., *Phys. Rev. Lett.* **32**, 879 (1974); J. Weiner, Ph.D. thesis, University of Massachusetts, Amherst, Massachusetts, 1974 (unpublished).
 - ¹⁵M. Ley-Koo and M. S. Green, *Phys. Rev. A* **16**, 2483 (1977).
 - ¹⁶M. R. Moldover, J. V. Sengers, R. W. Gammon, and R. J. Hocken, *Rev. Mod. Phys.* **51**, 79 (1979).
 - ¹⁷S. Jünger, B. Knuth, and F. Hensel, *Phys. Rev. Lett.* **55**, 2160 (1985).
 - ¹⁸R. E. Goldstein and N. W. Ashcroft, *Phys. Rev. Lett.* **55**, 2164 (1985).
 - ¹⁹A brief account of the major results described here has already appeared: R. E. Goldstein, A. Parola, N. W. Ashcroft, M. W. Pestak, M. H. W. Chan, J. R. de Bruyn, and D. A. Balzarini, *Phys. Rev. Lett.* **58**, 41 (1987).
 - ²⁰M. W. Pestak, Ph.D. thesis, The Pennsylvania State University, 1983; M. W. Pestak and M. H. W. Chan, *Phys. Rev. B* **30**, 274 (1984); *Bull. Am. Phys. Soc.* **29**, 227 (1984).
 - ²¹J. R. de Bruyn and D. A. Balzarini (unpublished).
 - ²²M. Burton and D. Balzarini, *Can. J. Phys.* **52**, 2011 (1974); D. Balzarini and M. Burton, *ibid.* **57**, 1516 (1979).
 - ²³W. J. Meath and R. A. Aziz, *Mol. Phys.* **52**, 225 (1984), and references therein.
 - ²⁴B. M. Axilrod and E. Teller, *J. Chem. Phys.* **11**, 299 (1943).
 - ²⁵E. E. Polymeropoulos, J. Brickmann, L. Jansen, and R. Block, *Phys. Rev. A* **30**, 1593 (1984).
 - ²⁶S. Baer and A. Ben-Shaul, *J. Chem. Phys.* **56**, 1238 (1972), consider the general case of higher-body interactions.
 - ²⁷L. Reatto and M. Tau, *Europhys. Lett.* **3**, 527 (1987).
 - ²⁸R. E. Goldstein and A. Parola, *Phys. Rev. A* **35**, 4770 (1987).
 - ²⁹B. Widom, *J. Chem. Phys.* **43**, 3898 (1965).
 - ³⁰J. S. Rowlinson, *Mol. Phys.* **52**, 567 (1984).
 - ³¹R. B. Griffiths and J. C. Wheeler, *Phys. Rev. A* **2**, 1047 (1970).
 - ³²M. E. Fisher, *Phys. Rev.* **176**, 257 (1968).
 - ³³J. S. Rowlinson and F. L. Swinton, *Liquids and Liquid Mixtures*, 3rd ed. (Butterworths, Boston, 1982), Chap. 3; see also J. M. H. Levelt-Sengers, *Ind. Eng. Chem., Fundam.* **9**, 470 (1970).
 - ³⁴D. A. McQuarrie, *Statistical Mechanics* (Harper and Row, New York, 1973), p. 304.
 - ³⁵G. Casanova, R. J. Dulla, D. A. Jonah, J. S. Rowlinson, and G. Saville, *Mol. Phys.* **18**, 589 (1970).
 - ³⁶O. Sinanoğlu, *Chem. Phys. Lett.* **1**, 340 (1967); *Adv. Chem. Phys.* **12**, 283 (1967).
 - ³⁷G. S. Rushbrooke and M. Silbert, *Mol. Phys.* **12**, 505 (1967).
 - ³⁸M. E. Fisher and J. S. Langer, *Phys. Rev. Lett.* **20**, 665 (1968).
 - ³⁹G. Stell and J. S. Høye, *Phys. Rev. Lett.* **33**, 1268 (1974).
 - ⁴⁰M. H. W. Chan, *Phys. Rev. B* **21**, 1187 (1980); M. W. Pestak and M. H. W. Chan, *Phys. Rev. Lett.* **46**, 943 (1981).
 - ⁴¹B. J. Thijsse, T. Doiron, and J. M. H. Levelt Sengers, *Chem. Phys. Lett.* **72**, 546 (1980).
 - ⁴²M. R. Moldover and R. W. Gammon, *J. Chem. Phys.* **80**, 528 (1984).
 - ⁴³R. F. Kayser, J. W. Schmidt, and M. R. Moldover, *Phys. Rev. Lett.* **54**, 707 (1985).
 - ⁴⁴M. J. Buckingham, in *Phase Transitions and Critical Phenomena*, edited by C. Domb and M. S. Green (Academic, London, 1972), Vol. 2, p. 1.
 - ⁴⁵C. Pittman, T. Doiron, and H. Meyer, *Phys. Rev. B* **20**, 3678 (1979).
 - ⁴⁶J. O. Hirschfelder, C. F. Curtiss, and R. B. Bird, *Molecular Theory of Gases and Liquids* (Wiley, New York, 1954).
 - ⁴⁷A. J. Guttman, *J. Phys. A* **8**, 1249 (1975).
 - ⁴⁸J. N. Israelachvili, *Intermolecular and Surface Forces* (Academic, New York, 1985), Chap. 4.
 - ⁴⁹G. R. Brown and H. Meyer, *Phys. Rev. A* **6**, 364 (1972).
 - ⁵⁰See studies discussed in Ref. 23.
 - ⁵¹F. W. Balfour, J. V. Sengers, M. R. Moldover, and J. M. H. Levelt Sengers, in *Proceedings of the Seventh Symposium on Thermophysical Properties*, edited by A. Cezairliyan (American Society of Mechanical Engineers, New York, 1977), pp. 786–92.
 - ⁵²F. Hensel (private communication) and unpublished.